How to cite: *Angew. Chem. Int. Ed.* **2024**, *63*, e202314028
doi.org/10.1002/anie.202314028

Inhibitors

Structure of *Staphylococcus aureus* ClpP Bound to the Covalent Active-Site Inhibitor Cystargolide A

Astrid Illigmann[#], Marie-Theres Vielberg[#], Markus Lakemeyer[#], Felix Wolf, Taulant Dema, Patrik Stange, Wolfgang Kuttenlochner, Elisa Liebhart, Andreas Kulik, Nicole D. Staudt, Imran Malik, Stephanie Grond, Stephan A. Sieber, Leonard Kaysser, Michael Groll,* and Heike Brötz-Oesterhelt**

Abstract: The caseinolytic protease is a highly conserved serine protease, crucial to prokaryotic and eukaryotic protein homeostasis, and a promising antibacterial and anticancer drug target. Herein, we describe the potent cystargolides as the first natural β-lactone inhibitors of the proteolytic core ClpP. Based on the discovery of two *clpP* genes next to the cystargolide biosynthetic gene cluster in *Kitasatospora cystarginea*, we explored ClpP as a potential cystargolide target. We show the inhibition of *Staphylococcus aureus* ClpP by cystargolide A and B by different biochemical methods in vitro. Synthesis of semisynthetic derivatives and probes with improved cell penetration allowed us to confirm ClpP as a specific target in *S. aureus* cells and to demonstrate the antivirulence activity of this natural product class. Crystal structures show cystargolide A covalently bound to all 14 active sites of ClpP from *S. aureus*, *Aquifex aeolicus*, and *Photorhabdus laumondii*, and reveal the molecular mechanism of ClpP inhibition by β-lactones, the predominant class of ClpP inhibitors.

Introduction

The highly conserved serine protease Clp is ubiquitous in prokaryotic cells and prokaryote-derived organelles of eukaryotic cells, representing a key player in the fundamental processes of protein quality control, proteostasis, and regulatory proteolysis.[1] A functional Clp protease complex comprises one or two sets of a hexameric Clp-ATPase and the tetradecameric proteolytic core ClpP containing 14 catalytic triads (Figure 1a). Both partners interact dynamically through conserved, flexible loops of the Clp-ATPase that insert into hydrophobic pockets of ClpP.[2a–c] Degradation-tag-carrying substrates are recognized by loops of the ATPase, and ATP-driven conformational changes fuel stepwise unfolding and translocation of the substrate into the proteolytic chamber of ClpP. The proteolytic activity of Clp proteases is regulated through specific recognition of substrates by the Clp-ATPases as well as through allosteric sites of ClpP. A hydrophobic pocket at the apical surface of ClpP (H-pocket) forms the major interaction site for the Clp-ATPases and allosterically activates the ClpP barrel by conformational control.[3] The substrate pockets of ClpP

[*] A. Illigmann,[#] E. Liebhart, A. Kulik, Dr. I. Malik, Prof. Dr. H. Brötz-Oesterhelt
Department of Microbial Bioactive Compounds, Interfaculty Institute of Microbiology and Infection Medicine, University of Tübingen
Auf der Morgenstelle 28, 72076 Tübingen (Germany)
E-mail: heike.broetz-oesterhelt@uni-tuebingen.de

Dr. M.-T. Vielberg,[#] W. Kuttenlochner, Prof. Dr. M. Groll
Chair of Biochemistry, Centre for Protein Assemblies, Technical University Munich
Ernst-Otto-Fischer-Strasse 8, 85748 Garching (Germany)
E-mail: michael.groll@tum.de

Dr. M. Lakemeyer,[#] Prof. Dr. S. A. Sieber
Chair of Organic Chemistry II, Technical University Munich, School of Natural Sciences, Center for Functional Protein Assemblies (CPA)
Ernst-Otto-Fischer-Straße 8/I, 85748 Garching b.München (Germany)

Dr. M. Lakemeyer[#]
Current address: Institute of Organic Chemistry and Macromolecular Chemistry, Friedrich Schiller University Jena
Humboldtstrasse 10, 07743 Jena (Germany)

Dr. F. Wolf, Dr. N. D. Staudt, Prof. Dr. L. Kaysser
Synthetic Biology of Anti-infective Agents, Pharmaceutical Institute, University of Tübingen
Auf der Morgenstelle 8, 72076 Tübingen (Germany)

T. Dema, P. Stange, Prof. Dr. S. Grond
Institute of Organic Chemistry, University of Tübingen
Auf der Morgenstelle 18, 72076 Tübingen (Germany)

Prof. Dr. L. Kaysser
Pharmazeutische Biologie, Institut für Wirkstoffentwicklung, Universitätsklinikum Leipzig
Eilenburger Strasse 15a, 04317 Leipzig (Germany)
E-mail: leonard.kaysser@uni-leipzig.de

Prof. Dr. H. Brötz-Oesterhelt
Cluster of Excellence Controlling Microbes to Fight Infections, University of Tübingen
Auf der Morgenstelle 28, 72076 Tübingen (Germany)

[#] co-first authors

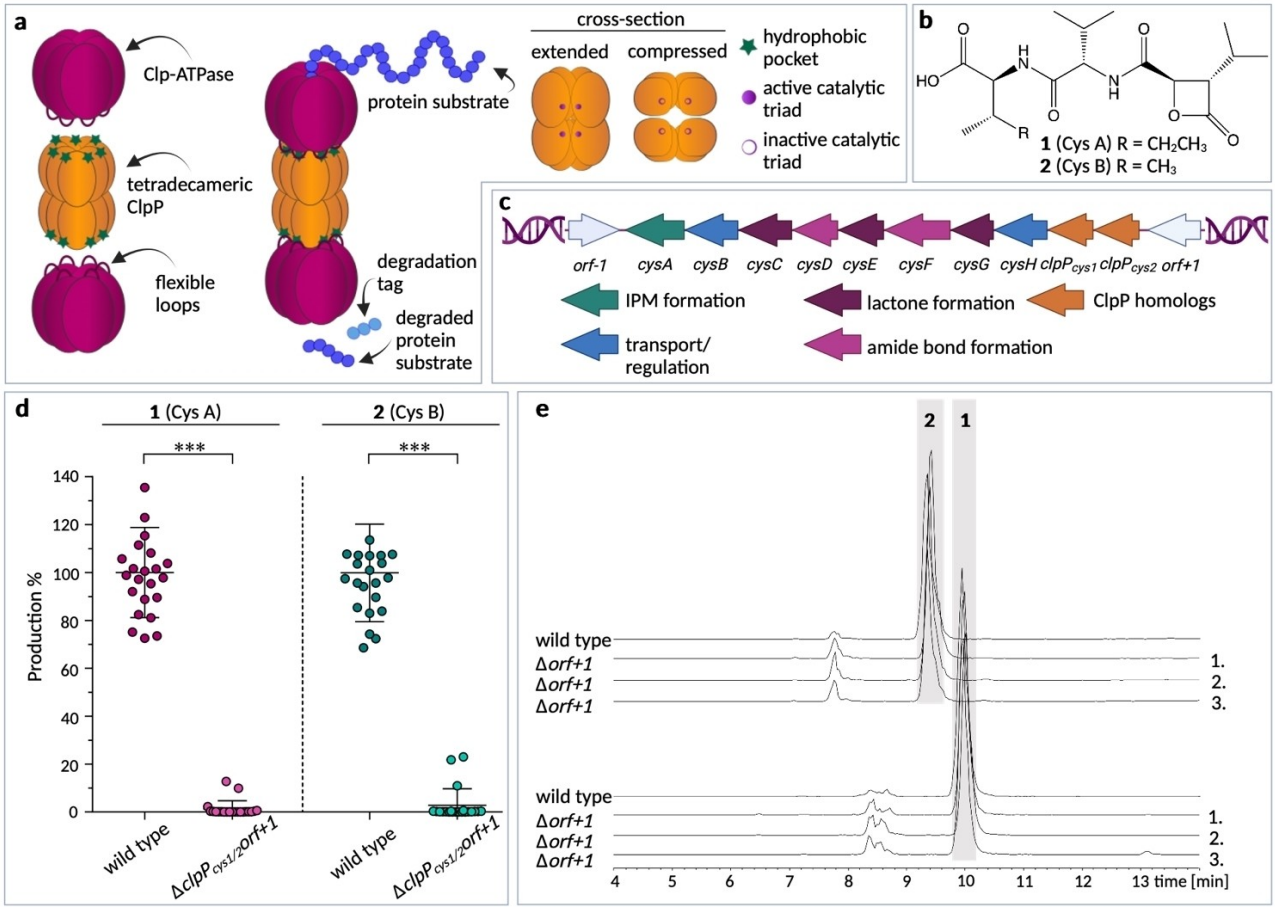

Figure 1. Analysis of the cystargolide biosynthetic gene cluster. a) Formation of an active proteolytic complex between the tetradecameric ClpP and a partner ATPase. The Clp-ATPase inserts via flexible loops into the hydrophobic pockets of ClpP. This active complex is able to recognize protein substrates with a specific tag and degrades them. The extended conformation of ClpP causes an optimal geometry for active-site residues, resulting in an active catalytic triad. In contrast, the compressed conformation of ClpP results in an unfavorable long distance between the active-site residues, resulting in an inactive catalytic triad. b) Structural representation of **1** (Cys A) and **2** (Cys B). c) Cystargolide biosynthetic gene cluster. $clpP_{cys1}$ and $clpP_{cys2}$ (highlighted in orange and previously designated *orf+1* and *orf+2*, respectively[10b]) are not involved in the biosynthesis of **1** (Cys A) and **2** (Cys B) as such but are required for efficient production. The 3-oxoacyl-ACP synthase located upstream of the *clpP* homologues and previously designated *orf+3* represents the new BGC border and is renamed *orf+1*. d) Statistical analysis of the production of **1** (Cys A) and **2** (Cys B) in *K. cystarginea* wild type (wt) and *K. cystarginea* $\Delta clpP_{cys1/2}orf+1$ demonstrates the requirement of the *clpP* homologues for efficient production; $n=44$, dots represent independent fermentations from 7 independent knockout clones; *** $p=0.005$ determined by t-test; mean, upper and lower quartiles are indicated. e) LC–MS analysis of *K. cystarginea* wt and three different clones of *K. cystarginea* $\Delta orf+1$ shows that deletion of the 3-oxoacyl-ACP synthase immediately upstream of the two *clpP* homologues does not impair cystargolide production (**2**=**2** (Cys B); **1**=**1** (Cys A)) and defines the new BGC boundary.

represent further allosteric sites where, in some bacteria, the transition to the active state was shown to be promoted by substoichiometric amounts of substrate mimics.[4a,b] ClpP conformation, plasticity and activity, including correct spatial alignment of the catalytic triads and the occurrence of substrate exit pores, is also influenced by the pH value within the proteolytic chamber.[5a,b] ClpP shifts dynamically between a compressed, inactive conformation, characterized by an unfavorably long distance between the active-site serine and the histidine side chain, and an extended, active conformation featuring an active-site geometry optimal for catalysis.[6a–d]

ClpP is a promising antibacterial and anticancer drug target, and ClpP modulators from different structural classes are being investigated and developed for therapeutic application.[7] Antibacterial acyldepsipeptides are prototype ClpP activators, competing with Clp-ATPases for the H-pockets of ClpP and deregulating the proteolytic core for Clp-ATPase-independent proteolysis. The anticancer imipridone class acts by the same mechanism.[8a–d] Among the various ClpP inhibitors described to date, the pioneering β-lactones play a central role, as they improved our understanding of the catalytic mechanism and demonstrated the anti-virulence potential of chemical ClpP inhibition. However, despite several in-depth mechanistic studies on synthetic β-lactones, which demonstrated their covalent attachment to the catalytic serine residue,[9a–c] a crystal structure has remained elusive, thereby precluding insight into the molecular binding mode and inhibition mechanism.

Cystargolides A (**1**) and B (**2**) are natural, β-lactone-containing secondary metabolites produced by the actinomycete *Kitasatospora cystarginea* NRRL B-16505. They possess a dipeptidic backbone and were previously described as 20S proteasome inhibitors.[10a–c] Interestingly, analysis of the cystargolide biosynthetic gene cluster (BGC) revealed the existence of two *clpP* genes, which were close to the biosynthetic genes but initially not included in the BGC.[10b] Inspired by this co-occurrence and considering the inhibition of ClpP by synthetic β-lactones, we revisited the role of these ClpP homologues in cystargolide biosynthesis and probed the potential of cystargolides for inhibiting ClpP.

Herein, we characterize the inhibition of ClpP by the cystargolides in detail, applying biochemical, chemical, and microbiological methods. Furthermore, we present the crystal structures of cystargolide A (**1**) bound to all 14 active sites of ClpP from *Staphylococcus aureus* (SaClpP, PDB ID 8OLL, 8R03), *Aquifex aeolicus* (AaClpP, PDB ID 8R04), and *Photorhabdus laumondii* (PlClpP, PDB ID 8R05) tetradecamers, revealing the molecular mode of inhibition. In addition, we prepared semisynthetic cystargolide derivatives with improved cell penetration. Our results complement the mechanistic understanding of the β-lactone action on ClpP.

Results and Discussion

ClpP Genes are Required for Efficient Cystargolide Production in *K. cystarginea*

We recently analyzed the biosynthesis of **1** (Cys A) and **2** (Cys B) and identified the *cysA-H* operon as the BGC for their production in *Kitasatospora cystarginea* NRRL B-16505 (Figure 1b, c). In this process, we noticed the presence of two *clpP* genes immediately upstream of the biosynthetic genes, which we annotated as *orf+1* and *orf+2* but did not include into the BGC, initially.[10b] However, the co-occurrence of *clpP* homologues next to the gene cluster for β-lactones motivated us to revisit their effect on cystargolide production. Knock-out of the two *clpP* genes plus an adjacent upstream gene abolished cystargolide production almost completely (Figure 1d; residual yield of **1** (Cys A) was 1.3 % (standard deviation (SD) 6.9 %) and of **2** (Cys B) was 2.8 % (SD 3.4 %) compared to the wild-type). In contrast, a mutant in which only the adjacent upstream gene was deleted showed full cystargolide production (Figure 1e). Thus, the two *clpP* homologues clearly contribute to cystargolide biosynthesis in *K. cystarginea* NRRL B16505 (Figure 1c). This finding implies a role for those ClpP proteins as self-protection factors, supporting the producer strain against the activity of the cystargolides **1** (Cys A) and **2** (Cys B), and we thus propose to rename them $clpP_{cys1}$ and $clpP_{cys2}$.

Cystargolides are Covalent Inhibitors of the Active-Site Serine of S. aureus ClpP

To investigate the potential of **1** (Cys A) and **2** (Cys B) for ClpP inhibition, we carried out various biochemical analyses. Since synthetic β-lactones were shown to covalently bind the active-site serine of proteases,[9a] we used intact protein mass spectrometry to probe wildtype ClpP (SaClpP wt) and a loss of function mutant ($SaClpP_{S98A}$) for covalent binding of **1** (Cys A) and **2** (Cys B) to the catalytic Ser98 (Figure 2a). Upon treatment with **1** (Cys A), 100 % of SaClpP wt displayed a mass shift of 370.2 Da, corresponding to SaClpP covalently bound to the compound (Δobs 370.2 Da, Δcalc 370.2 Da). The $SaClpP_{S98A}$ mutant was not modified, proving the catalytic serine as the site of attack (Figure 2a). In the case of **2** (Cys B), 83 % of the active-site serines were modified, indicated by a mass shift of 356.0 Da (Δobs 356.0 Da, Δcalc 356.2 Da; Figure 2a). Next, we quantitatively assessed the inhibitory potency of **1** (Cys A) and **2** (Cys B) on SaClpP in biochemical substrate degradation assays. Using the peptide substrate Suc-LY-AMC, we recorded the fluorescence generated upon peptide hydrolysis and compared degradation kinetics in the absence and presence of **1** (Cys A) and **2** (Cys B). Inactivation rates (k_{obs}/[I] values) were calculated with k_{obs} representing the observed rate constant for the binding of an inhibitor [I].[9c] This method is commonly used to reliably determine the potency of covalent inhibitors independent of the incubation time, with higher values indicating faster and more efficient binding. Both cystargolides demonstrated high k_{obs}/[I] values indicative of high affinity for ClpP, with **2** (Cys B) (k_{obs}/[I] 656.4 ± 94.5 $M^{-1}s^{-1}$) binding to SaClpP slightly faster than **1** (Cys A) (k_{obs}/[I] 285.5 ± 72.2 $M^{-1}s^{-1}$; Figure 2b). Since cystargolides were initially described as proteasome inhibitors,[10a] we also determined k_{obs}/[I] values for both natural cystargolides on the human 20S proteasome. Sixfold lower k_{obs}/[I] values were calculated for **1** (Cys A) (79.2 ± 29.5 $M^{-1}s^{-1}$) and **2** (Cys B) (51.5 ± 4.6 $M^{-1}s^{-1}$; Figure S3). These substantially lower k_{obs}/[I] values suggest a slower binding to the proteasome than to SaClpP. However, the different assay conditions required for the enzymes preclude a direct comparison of the values.

For synthetic β-lactones two principal mechanisms of ClpP inhibition have previously been described. The first mechanism is based on the quantitative covalent inactivation of all active-site serines within the tetradecamer, while the second mechanism is characterized by the de-oligomerization of ClpP, even if the active sites are only partially modified.[11] For instance, the synthetic β-lactone D3 modified all 14 active sites of SaClpP without changing the oligomeric state, whereas E2 induced heptamer formation with only 35 % of Ser98 modification.[11] Thus, we next analyzed the state of oligomerization of SaClpP upon cystargolide binding using size exclusion chromatography (Figure 2c). As SaClpP retained the tetradecameric state after incubation with the inhibitor, we conclude that cystargolides act by the first mechanism. For a comprehensive picture, we also analyzed the impact of the cystargolides on SaClpXP, i.e., the proteolytic core ClpP interacting with

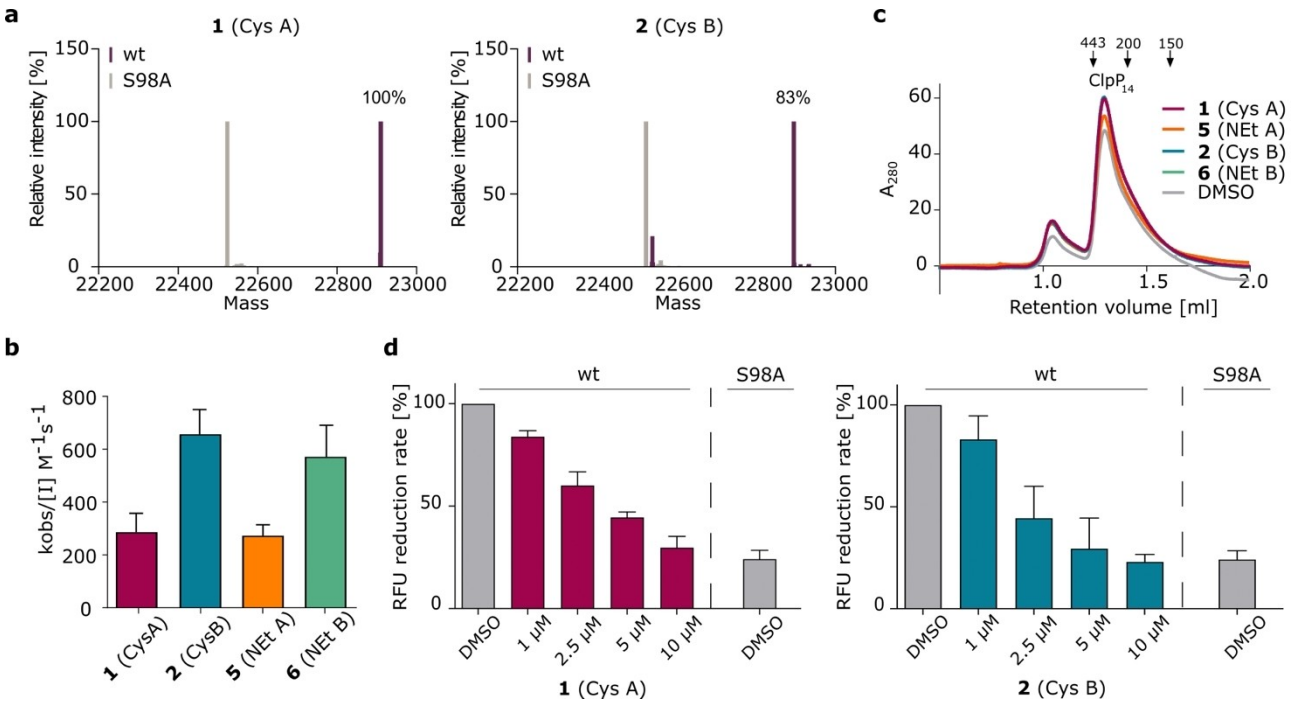

Figure 2. Biochemical analyses of the cystargolides. a) Intact protein mass-spectrometry to analyze the covalent binding of the natural products **1** (Cys A) (Δ_{obs} = 370.2 Da) and **2** (Cys B) (Δ_{obs} = 356.0 Da) to SaClpP wt and the active-site mutant $SaClpP_{S98A}$. The percentage of modified Ser98 is indicated above the respective mass peaks of the adduct. b) Inactivation rates (k_{obs}/[I] values) for **1** (Cys A) 285.5 ± 72, **2** (Cys B) 656.4 ± 94, **5** (NEt A) 272.4 ± 42 and **6** (NEt B) 571.1 ± 120 and SaClpP. Also included in (b) for comparison are semisynthetic ethyl amide congeners of the natural products, which are introduced later in the text and were generated to improve cell penetration: k_{obs}/[I] values for **5** (NEt A, derivative of **1** (Cys A)) 272.4 ± 42 and **6** (NEt B, derivative of **2** (Cys B)) 571.1 ± 120 (see Figure 6a for chemical structures). k_{obs}/[I] values are derived from two biological experiments (i.e., different cystargolide and ClpP preparations tested on different days) with three technical replicates per concentration and are shown as mean ± SD. c) Size-exclusion chromatograms displaying the integrity of the SaClpP-tetradecamer upon incubation with **1** (Cys A), **2** (Cys B), **5** (NEt A) and **6** (NEt B). DMSO was used as a control. One representative experiment for each compound is shown from three replicates (molecular weight markers: 443 kDa: apoferritin, 200 kDa: β-amylase, 150 kDa: alcohol-dehydrogenase, detection was carried out at A_{280}). For replicate experiments see Figure S4. d) Inhibition of SaClpXP proteolytic activity (SaClpX: 4 µM, SaClpP: 2 µM) during degradation of ssrA-eGFP by **1** (Cys A) and **2** (Cys B). The reduction rate of eGFP-ssrA fluorescence (in relative fluorescence units, RFU) by uninhibited ClpXP (DMSO control) was set to 100% and of an aliquot containing eGFP-ssrA but neither ClpP nor ClpX to 0%. As observed previously (e.g., in[3]) ClpX contributes to RFU reduction in this assay by eGFP-ssrA unfolding without proteolysis. Therefore, even a complete lack of the catalytic function of ClpP, as demonstrated here by exchanging wt ClpP for its catalytic triad mutant ($SaClpP_{S98A}$), could not reduce the RFU reduction rate to 0%. Each data set represents two biological experiments with three technical replicates per concentration and is shown as mean ± SEM (standard error of mean). Data are normalized to DMSO as a control (100% activity).

the cognate Clp-ATPase ClpX for protein hydrolysis. To this end, we monitored the degradation of ssrA-tagged eGFP, an established model ClpXP-substrate, by fluorescence decrease. Both cystargolides efficiently interfered with protein degradation in a concentration-dependent manner and at the highest concentration tested (10 µM) the effects of the cystargolides matched the effect of the active-site serine mutant $SaClpP_{S98A}$ (Figure 2d).

Validation of ClpP as a Preferential Target of Cystargolides in S. aureus Cells

To confirm ClpP as a target of cystargolides in *S. aureus* cells in vivo, we performed activity-based protein profiling (ABPP). This method represents a chemical proteomics approach that probes nucleophilic active sites of enzymes in living cells for the binding of electrophilic probes derived from an inhibitor of interest.[12] Individual stereochemical characteristics of the inhibitor determine the target preference. To this end, we synthesized the two cystargolide probes **3** (ML292) and **4** (ML293) (Figure 3a), in which alkyne tags were introduced by amidation of the carboxylic acid group of **1** (Cys A) and **2** (Cys B), respectively. At first, living cells are incubated with an alkyne-functionalized probe (Figure 3b) or, in case of competition assays, first with the inhibitor itself and then with the probe (Figure 3c). The compounds enter the cells and covalently bind to their target enzymes. Samples are analyzed using either fluorescence SDS-PAGE or, after enrichment through the biotin tag, via protein mass spectrometry (MS) workflows (Figure 3b,c).

Intact protein mass spectrometry confirmed covalent binding of the probes to purified SaClpP in vitro. Both probes induced a mass shift in SaClpP wt, with **3** (ML292) modifying 94% and **4** (ML293) binding 80% of the enzyme (Figure S1). Next, we evaluated probe efficiency and

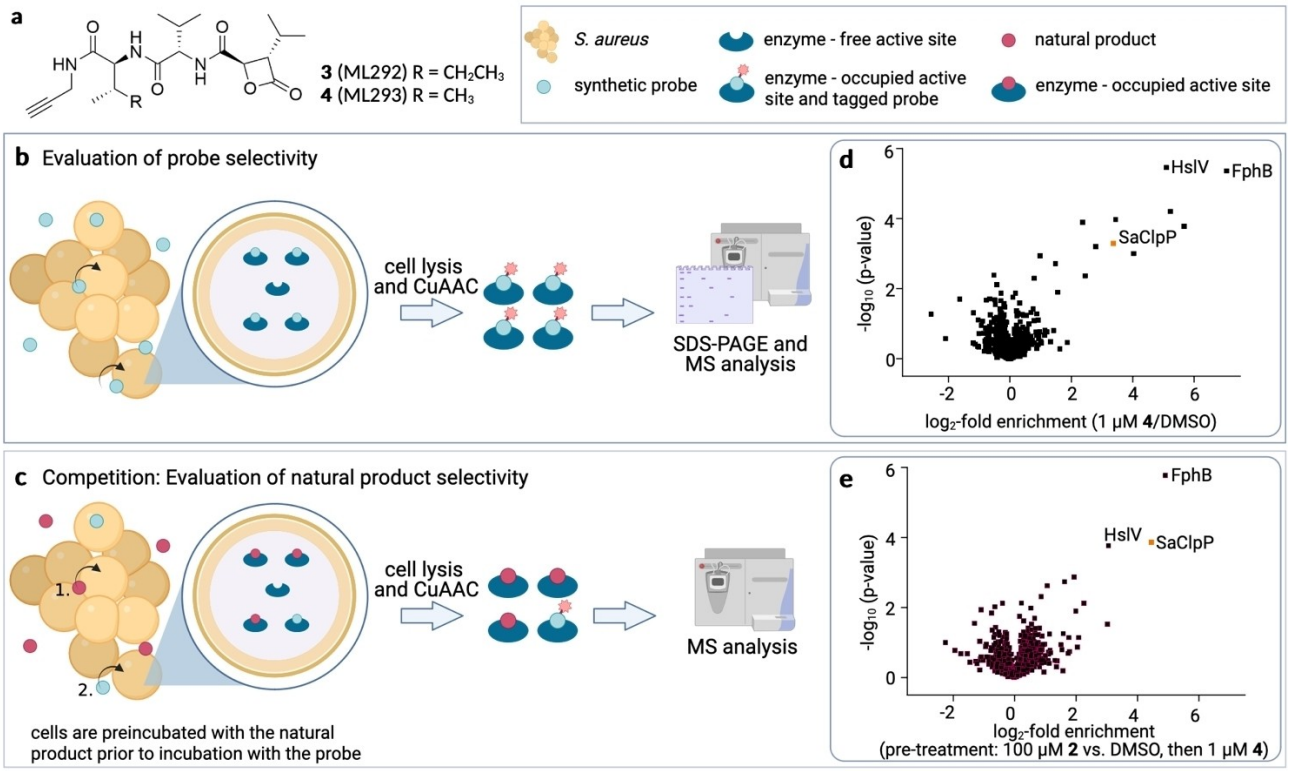

Figure 3. Activity-based protein profiling (ABPP) studies in *S. aureus*. a) Structures of the cystargolide-based probes **3** (ML292) derived from **1** (Cys A), and **4** (ML293) derived from **2** (Cys B). b) Workflow of the ABPP method for evaluating activity-based probe selectivity. Intact bacterial cells are treated with probes covalently binding to protein targets. Cells are lysed, and for downstream analysis a fluorophore- or affinity-tag is attached to the probe through click chemistry (copper-catalyzed azide-alkyne cycloaddition (CuAAC)). Fluorescent SDS-PAGE analysis is used for the analytical assessment of protein targets. Preparative ABPP for target identification is conducted by MS analysis of enriched and trypsin-digested affinity-labeled proteins. c) Workflow of the ABPP method for evaluation of inhibitor selectivity. Before incubation with the probe, cells are preincubated with the parent inhibitor compound. d) Volcano plot representation of enriched protein targets for ABPP experiments with 1 µM **4** (ML293) vs. DMSO. e) Volcano plot representation of ABPP competition experiments with exposure of cells to 100 µM **2** (Cys B) or DMSO prior to labeling with 1 µM **4** (ML293). SaClpP, FphB, and HslV stand out as the most enriched targets of **2** (Cys B). Data are derived from four biological replicates for each labeling condition. For denomination of all enriched proteins, see Figure S6.

selectivity in intact *S. aureus* cells on an analytical scale by SDS-PAGE. Increasing probe concentrations (1, 3, 10, 30 µM) were applied to *S. aureus* NCTC 8325. After cell lysis, a rhodamine azide tag (Rh-N_3) was added through copper-catalyzed click chemistry for fluorescent detection. Both probes labeled ClpP efficiently within *S. aureus* cells, and ClpP appeared as the only prominently labeled protein band on the gel (Figure S5). Probe **4** (ML293) performed slightly better than **3** (ML292), and 1 µM of **4** (ML293) was sufficient for effective SaClpP labeling (Figure S5). Thus, we selected **4** (ML293) and the corresponding natural product **2** (Cys B) for preparative ABPP and analysis by mass spectrometry. First, we determined which proteins were labeled by directly incubating *S. aureus* cells with probe **4** (ML293) (Figures 3d and S6a,c). Next, we performed a competition experiment in which the cells were treated with the natural product **2** (Cys B) to saturate all targets before exposure to probe **4** (ML293) (Figures 3e and S6b,c). Whereas several enzymes were labeled by **4** alone (ML293, Figure 3a), only a few proteins were detected after pre-incubation with **2** (Cys B) (Figure 3e). These proteins represent the covalently modified cellular targets of the parent natural product **2** (Cys B). Among them the most prominent was SaClpP, followed by the serine hydrolase FphB (Q2FV90), which belongs to the subgroup of α,β-hydrolases and was shown to process C4–C8 fatty acid esters in vitro as a carboxylic esterase.[13] Interestingly, FphB is an important virulence factor for the infection of heart and liver tissues in a mouse model of systemic *S. aureus* infection.[13] In addition, the ATP-dependent protease subunit HslV (Q2FZ29), was significantly, albeit less strongly, enriched (Figure 3e). Consequently, using the competition approach of ABPP, we were able to show that **2** (Cys B) bound two hydrolases relevant for virulence of *S. aureus* cells, on the one hand the key virulence regulator ClpP and on the other hand FphB. While FphB activity was observed in the exponential and stationary phases of growth in liquid culture,[13] ClpP regulates virulence predominantly in the post-exponential and stationary phases of bacterial growth.[14] By potentially targeting FphB besides ClpP, the cystargolides might be capable of attenuating the virulence of *S. aureus* by a two-pronged approach, i.e., by inhibiting two virulence factors expressed at different stages of bacterial growth.

Hla-expression in *S. aureus* Is Abolished by a Cystargolide Derivative

Pathogenic *S. aureus* strains secrete a variety of virulence factors, including extracellular proteases and α-hemolysin. The ClpXP protease complex promotes α-hemolysin (*hla*) production and Δ*clpP* mutants show reduced *hla* expression.[14,15] A reduction of *hla* expression can also be induced by chemical inhibition of SaClpP, as shown for synthetic β-lactones.[9a,b] To examine the impact of cystargolides on α-hemolysin production, *S. aureus* NCTC 8325-4 wt and an isogenic Δ*clpP* mutant were exposed to the cystargolides in an agar-based assay (Figure 4). The reduced *hla* production and hence the reduced α-hemolysin secretion by the Δ*clpP* mutant result in a reduced hemolysis zone on sheep blood agar, i.e., the red blood cells remain intact.

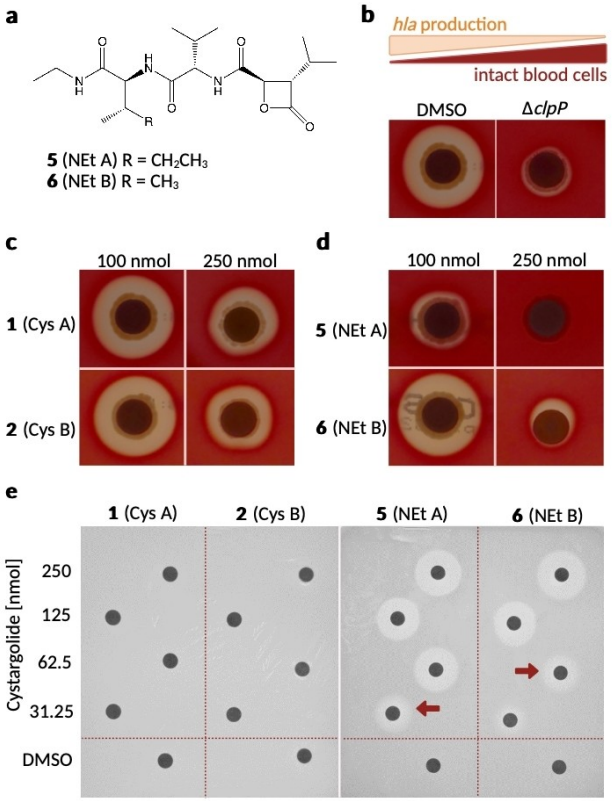

Figure 4. Antimicrobial activity of **1** (Cys A), **2** (Cys B), **5** (NEt A), and **6** (NEt B) against *S. aureus* 8325-4 and *S. griseus* Waksman. a) Structure of the cystargolide derivatives **5** (NEt A) and **6** (NEt B). b) Impact of ClpP on Hla production and the corresponding lysis of red blood cells. In the hemolysis assay, DMSO served as solvent control, allowing Hla production, which manifests as an erythrocyte-lysis zone around the filter paper. In contrast, *hla* production is attenuated in the Δ*clpP* mutant, which was used as a positive control for inhibition *of* Hla production. c) *S. aureus* hemolysis in the presence of either natural product **1** (Cys A) or **2** (Cys B) at 100 nmol or 250 nmol. d) *S. aureus* hemolysis in the presence of either the ethylamide congener **5** (Net A) or **6** (NEt B), at 100 nmol and 250 nmol. e) Effect of increasing concentrations of **1** (Cys A), **2** (Cys B), **5** (NEt A), and **6** (NEt B) on the growth of *S. griseus*. Red arrows point to comparable growth inhibition. One representative experiment out of two independent biological replicates is shown.

Compared to DMSO-treated cells (negative control), 250 nmol of the natural products **1** (Cys A) and **2** (Cys B) only moderately decreased the diameter of the hemolysis zone (Figure 4b,c). Hypothesizing that this mild effect could be due to low cell entry rather than target affinity and that the carboxy moiety might hamper the passage of **1** (Cys A) and **2** (Cys B) across the cytoplasmic membrane, we prepared the more hydrophobic *N*-ethylamide cystargolides NEtA (**5**) and NEtB (**6**). These congeners inhibited α-hemolysin production in *S. aureus* efficiently at doses of 250 nmol, with **5** (NEt A) leading to almost complete inhibition at 100 nmol (Figure 4d). The inhibitory activity of **5** (NEt A) and **6** (NEt B) against purified SaClpP was well retained (Figure 2b). With respect to inhibition of peptide hydrolysis, both derivatives mirrored the $k_{obs}/[I]$ values of the natural products (Figure 2b). Thus, the stronger anti-hemolysis effect of the ethylamides **5** (NEt A) and **6** (NEt B) compared to natural cystargolides **1** (Cys A) and **2** (Cys B) presumably originates from improved cell entry. While inhibiting the virulence of *S. aureus*, cystargolide treatment did not prevent bacterial growth, since ClpP is not essential in this microorganism in vitro. In contrast, streptomycetes depend on ClpP function for viability. To probe for an antibacterial effect of the cystargolides, we tested the compounds against *Streptomyces. Streptomyces coelicolor* possesses 5 tightly regulated *clpP* genes, i.e., *clpP1, clpP2, clpP3, clpP4*, and *clpP5*,[16] and the heteromeric tetradecamer ClpP3P4 had previously been shown to be insensitive against synthetic β-lactones.[17] In contrast, *Streptomyces griseus* Waksman naturally lacks *clpP3* and *clpP4*.[16] When we tested the cystargolides **1** (Cys A) and **2** (Cys B) against *S. griseus*, both natural products showed no effect (Figure 4e). However, the ethylamides **5** (NEt A) and **6** (NEt B) showed concentration-dependent growth inhibition, with **5** demonstrating again a stronger effect at low concentrations than **6** (Figure 4e). These results confirm cell penetration as an obstacle for the natural cystargolides and demonstrate that the amidation towards the more hydrophobic ethylamide-moiety facilitates membrane penetration and growth inhibition in *S. griseus*.

Molecular Inhibition Modes for Bacterial ClpPs and the Yeast 20S Proteasome

To elucidate the binding mode of cystargolides to ClpP and the mechanism of inhibition, we solved the X-ray structures of **1** (Cys A) in complex with ClpP (Table S3) from *S. aureus* (PDB ID 8OLL, 8R03), *A. aeolicus* (PDB ID 8R04), and *P. laumondii* (PDB ID 8R05). The crystallographic analyses revealed that each ClpP:**1** (Cys A)-complex adopts an extended conformation of all H5-helices. Thereby, the aspartate/arginine oligomeric sensor is perfectly aligned, while different orientations of the catalytically active histidine indicate some flexibility at the active site (Figure S9). The strong positive difference in electron density observed at the reactive centers of each ClpP subunit confirmed binding of **1** (Cys A) (Figure 5a). Focusing on SaClpP at 2.0 Å resolution (PDB ID 8R03), the peptide-like

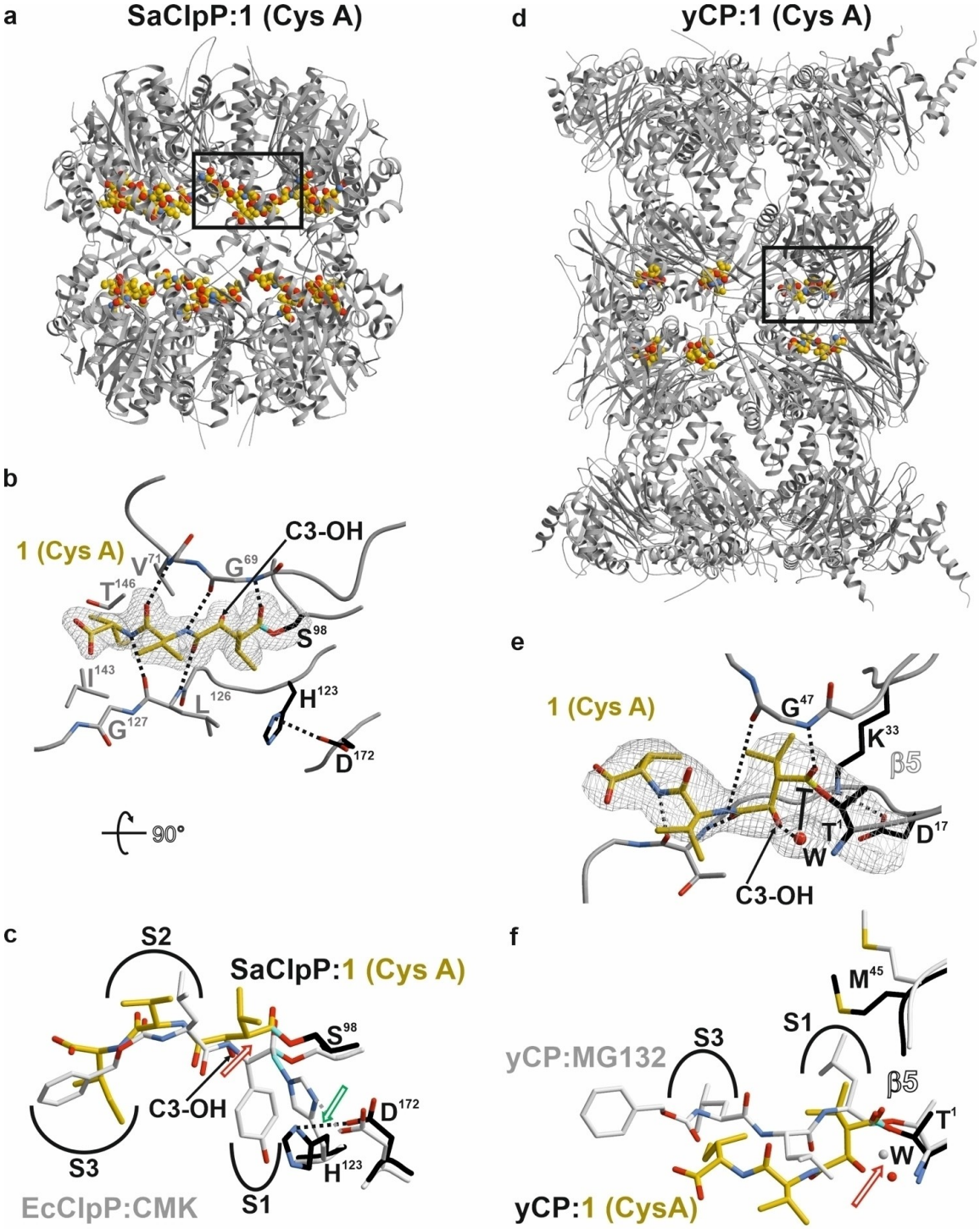

Figure 5. Crystal structures of ClpP from *S. aureus* (SaClpP, PDB ID 8R03) and yeast 20S proteasome core particle (yCP, PDB ID 8OLR) in complex with the natural product **1** (Cys A). a) Structure of SaClpP bound to **1** (Cys A) (spheres, carbon atoms in gold, oxygen in red, nitrogen in blue). The black rectangle marks the zoomed area. b) $2F_o$-F_c electron density map (gray mesh; contoured to 1σ) of **1** (Cys A) bound to the active-site nucleophile Ser98Oγ of SaClpP. The covalent linkage to Ser98 is colored in cyan, and residues of the catalytic triad (His123, Asp172) are indicated (H-bonds are shown as dotted lines). c) Structural superposition of **1** (Cys A) bound to SaClpP with a peptide chloromethyl ketone (CMK, carbon atoms are shown in gray) in complex with ClpP from *E. coli* (EcClpP, PDB 2FZS).[19] Non-primed specificity (S) pockets of the enzymes are highlighted in black. Note that the P1 sites of the two inhibitors differ in their position owing to the *S*-configuration of the isopropyl side chain in **1** (Cys A) (red arrow), and the orientation of His123 in the bound state (green arrow). d) Complex structure of yCP with the distinct α- and β-subunits colored in gray. e) $2F_o$-F_c electron density map of **1** (Cys A) bound to the Thr1O$^{\gamma}$ of subunit β5. The water molecule is shifted by 1 Å from the Bürgi-Dunitz trajectory inhibiting ester-bond hydrolysis (highlighted in black). f) Structural superposition of **1** (Cys A) with the peptide aldehyde Z-Leu-Leu-Leu-aldehyde (MG132, carbon atoms are shown in gray, PDB ID 4NNN).[20] Both ligands are covalently bound to Thr1O$^{\gamma}$ of subunit β5. The displacement of the nucleophilic water molecule is marked by a red arrow.

scaffold occupies the substrate binding channel, and the warhead is covalently bound to the nucleophile Ser98 in the active site through an ester bond that results from the opening of the β-lactone ring (Figure 5b). The hydroxy group (C3–OH) of **1** (Cys A), generated upon covalent linkage to the active-site serine, lacks any coordination, whereas the carbonyl oxygen atom is stabilized by Gly69NH. Hydrogen bonds between the inhibitor main chain atoms and Leu126NH, Gly69O, Val71NH, and Leu126O are typical of an antiparallel β-sheet. The P2 valine residue is solvent-exposed, while the P3 isoleucine group is coordinated to Val71, Ile143, and Thr146. However, crucial for the inhibitory mechanism of **1** (Cys A) is the P1-isopropyl group at the β-lactone ring. Owing to its *S*-configuration, which here is inverted compared to natural proteinogenic L-amino acids, the S1 specificity pocket is only partially occupied. Nevertheless, the P1 site undergoes strong van der Waals interactions with Leu126. This characteristic interplay hinders the attack of a nucleophilic water molecule and the release of **1** (Cys A) from the active site, thus explaining its inhibitory effect. More specifically, the Bürgi-Dunitz trajectory,[18] which describes the angle required for nucleophilic attack on a carbonyl carbon atom, is blocked, and deacylation of the ester bond can no longer occur (Figure 6a; for comparison of the reaction mechanism with a peptide substrate see Figure S7). The unusual orientation of the P1-alkyl side chain is illustrated by the overlay with ClpP bound to a peptide chloromethyl ketone (CMK) inhibitor (Cbz-Leu-Tyr-CMK, PDB 2FZS)[19] (Figure 5c). CMK exerts its inhibitory effect by forming a tetrahedral intermediate that covalently links His123 to the ligand (Figure S8). Compared to the P1-tyrosine residue of the synthetic dipeptide CMK, the *S*-configuration at P1 of **1** (Cys A) prevents side chain rotations by 180° (Figure 5c). Moreover, the P2 (Val) and P3 (Ile) residues of **1** (Cys A) are shifted by one carbon atom compared to Cbz-Leu-Tyr-CMK as well as natural peptide substrates. Thus, the particular architecture of **1** (Cys A) allows the formation of a stable antiparallel β-sheet. In addition, binding of **1** (Cys A) displaces His123 resulting in a misaligned catalytic triad which might contribute to the inhibitory effect. Notably, the terminal carboxy group of the natural product does not interact with protein residues and points toward the central chamber of ClpP. This feature explains why derivatizing this position to form the ethylamides **5** (NEt A) and **6** (NEt B) did not interfere much with the inhibitory activity and invites further synthetic exploration to improve the drug-like properties of this structural class in future studies.

To compare the binding mode of **1** (Cys A) to ClpP with the initially reported target,[12] the 20S proteasome core particle (CP), we determined the X-ray structure of yeast CP (yCP) in complex with **1** (Cys A) at 2.8 Å resolution (PDB ID 8OLR, Table S3; Figure 5d). The electron density map displayed **1** (Cys A) covalently bound to all active β subunits (β1, β2, and β5), as high ligand concentrations (>20 mM) were used for crystal soaking. However, because cystargolides lack strong interactions with protein residues in the caspase- (β1) and trypsin-like (β2) binding channels,

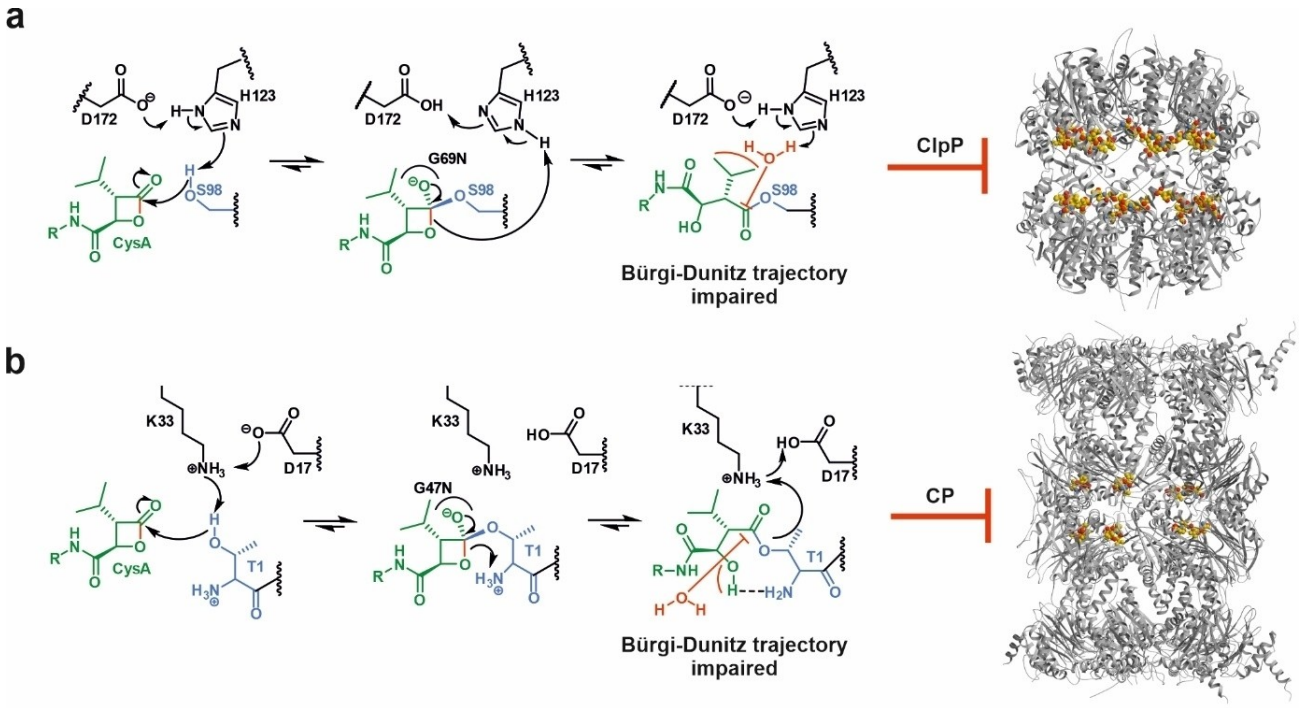

Figure 6. Proposed mechanism for the inhibition of a) ClpP proteases or b) 20S proteasomes (CPs) by cystargolides. Although the natural product is covalently bound to both protein complexes through an ester bond, there are striking differences in the mode of action. In ClpP, the *S* configuration of the P1-isopropyl side chain blocks binding of the nucleophilic water molecule, whereas in CP the generated hydroxy group of the ligand prevents hydrolysis.

the F_O-F_C map for the ligand is diffuse at these sites. By contrast, **1** (Cys A) is well defined in the chymotrypsin-like β5 subunit (Figure 5e), which is in agreement with the low IC_{50} value of 0.36 μM measured for inhibition of the β5 proteolytic activity[10a] and the previously described yCP:**2** (Cys B) complex structure (PDB 6G7F).[10c] Similar to the nucleophilic attack of Ser98 in SaClpP, Thr1O$^{\gamma}$ of β5 attacks the carbonyl carbon atom of the β-lactone ring, causing opening of the ring and covalent attachment of **1** (Cys A) to the proteasomal active site through an ester bond. As observed for ClpP, the ligand aligns along the substrate binding channel by forming an antiparallel β-sheet and the acyl group is H-bonded with the oxyanion hole formed by Gly47NH. Hydrolysis of **1** (Cys A) from β5 is prevented by the C3-OH hydroxyl group that is generated upon lactone opening and displaces the nucleophilic water molecule from the Bürgi-Dunitz trajectory (Figure 6b). The structural overlay of **1** (Cys A) bound to β5 with the proteasome inhibitor MG132 (PDB 4NNN)[20] shows similar H-bond interactions of the acyl-oxygen atom with Gly47NH, even though the sp^2-hybridized ester of **1** (Cys A) does not mimic tetrahedral intermediate-like peptide aldehydes such as MG132 (Figure 5f). In summary, inhibition of ClpPs or proteasomes by cystargolides requires the unusual stereochemistry of the P1 site and the α-hydroxyamide group which significantly differs from an amide-bond of natural peptide substrates.

Conclusion

Various ClpP modulators have been reported, ranging from ClpP activators, such as ADEP, to inhibitors, such as β-lactones, phenyl esters, and the recently described clipibicyclene.[8d,9c,21a–c] The cystargolides **1** (Cys A) and **2** (Cys B) represent the first described β-lactone inhibitors of ClpP discovered from nature and the first β-lactones for which ClpP co-crystal structures have been solved. Cystargolide is covalently bound to all active sites of ClpPs from different organisms, including gram-positive (*S. aureus*), thermophilic (*A. aeolicus*) and gram-negative (*P. laumondii*) bacteria, stabilizing the protease in the extended state. Suicide inhibition is obtained through structural mimicry of a natural peptide substrate. The peptide-like scaffold of cystargolide occupies the substrate binding channel, and the cleaved β-lactone warhead is covalently ester-linked to the active-site serine. Crucial for the inhibitory mechanism of cystargolide is the *S*-configuration of the P1-isopropyl group at the β-lactone ring, which is inverted compared to proteinogenic L-amino acids and sterically hinders the attack of a nucleophilic water molecule for enzyme regeneration. The second important inhibitory feature is the adjacent α-hydroxyamide group, which significantly differs from an amide bond of natural peptide substrates.

The two *clpP* genes located next to the biosynthetic machinery of the cystargolides in *K. cystarginea* led us to identify ClpP as a natural target of this compound class. Likewise, resistance-mediating *clpP* genes are associated with the BGC of clipibicyclene in *Streptomyces cattleya*, and target-directed genome mining revealed that clipibicyclene belongs to a large family of ClpP-associated BGCs, spreading across bacterial phyla.[21c] Although initially overlooked, Clp modulators seem to be common in nature.

ClpP and Clp ATP-ases are currently being pursued as drug targets in several lead optimization programs based on natural, semisynthetic, and synthetic modulators.[7,8a,22a–d] Inhibition of the Clp protease is a promising anti-virulence and anti-mycobacterial strategy, while activation and dysregulation of ClpP have been shown to inhibit bacterial and tumour proliferation in preclinical and clinical studies, respectively.[7,23] The observation that cystargolides can be modified to improve bacterial-cell penetration warrants further exploration.

Author Contributions

Conceptualization of study and manuscript: A. I., H.B.-O.; fermentation, compound purification and analytics: F.W., A.K., E.L., L.K.; Enzyme assays: A.I. and E.L. Clp protease, N.D.S. proteasome; synthesis of probes and derivatives: M.L., T.D., P.S., S.G., S.A.S.; Proteomics: M.L., S.A.S.; in vivo assays and producer strain knock-outs: A.I., F.W., E.L., H.B-O; structure elucidation: M.-T.V., W.K., M.G.; writing of the original draft: A.I., F.W., I.M. and H.B-O.; writing of methods section: A.I., M.G., W.K., M.L., F.W., N.D.S., T.D.; final visualization of figures and assembly of the manuscript: A.I.; review and editing of the manuscript, A.I. and H.B.-O.; funding acquisition, S.G., S.A.S., M.G., L.K., H.B.-O.; all authors have read and agreed to the published version of the manuscript.

Acknowledgements

We thank all members of our teams for their support and critical discussions, Libera Lo Presti for critically reading the manuscript and Martin Köllen for technical support. Funding is acknowledged by the Deutsche Forschungsgemeinschaft (German Research Foundation, DFG), within the TRR 261, Project-ID: 398967434 to A.I., E.L. and H.B-O., DFG grant No. 1861/10-3 to M.-T.V., W. K., and M.G. (A02), DFG grant CRC1035, project 201302640 to S.A.S. (A09) as well as KA 3071/4-1 and KA 3071/6-1 to L.K. We thank the staff of the beamline X06SA at the Paul Scherrer Institute, Swiss Light Source, Villigen Switzerland for assistance during data collection, and acknowledge funding from the European Community's Seventh Framework Programme (FP7/2007-2013) under BioStruct-X (grant agreement no. 283DFG grant CRC). M.L. was supported by the German National Academic Foundation. L.K., S.G. and H.B.-O. acknowledge infrastructural support by the Cluster of Excellence EXC2124 "Controlling Microbes to Fight Infection", Project-ID: 390838134. N.D.S. and L.K. acknowledge support by the Institutional Strategy of the University of Tübingen (DFG, ZUK 63). Open Access funding enabled and organized by Project DEAL Open Access funding enabled and organized by Projekt DEAL.

Conflict of Interest

The authors declare no conflict of interest.

Data Availability Statement

The data that support the findings of this study are available in the supplementary material of this article.

Keywords: Anti-Virulence · Caseinolytic Protease · Inhibitors · Natural Products · Protein Crystallography

[1] A. Illigmann, Y. Thoma, S. Pan, L. Reinhardt, H. Brötz-Oesterhelt, *Microb. Physiol.* **2021**, *31*, 260–279.
[2] a) M. F. Mabanglo, W. A. Houry, *J. Biol. Chem.* **2022**, *298*, 101781; b) Z. A. Ripstein, S. Vahidi, W. A. Houry, J. L. Rubinstein, L. E. Kay, *eLife* **2020**, *9*, e52158; c) C. Gatsogiannis, D. Balogh, F. Merino, S. A. Sieber, S. Raunser, *Nat. Struct. Mol. Biol.* **2019**, *26*, 946–954.
[3] M. Gersch, K. Famulla, M. Dahmen, C. Göbl, I. Malik, K. Richter, V. S. Korotkov, P. Sass, H. Rübsamen-Schaeff, T. Madl, H. Brötz-Oesterhelt, S. A. Sieber, *Nat. Commun.* **2015**, *6*, 6320.
[4] a) T. Akopian, O. Kandror, R. M. Raju, M. Unnikrishnan, E. J. Rubin, A. L. Goldberg, *EMBO J.* **2012**, *31*, 1529–1541; b) S. Vahidi, Z. A. Ripstein, J. B. Juravsky, E. Rennella, A. L. Goldberg, A. K. Mittermaier, J. L. Rubinstein, L. E. Kay, *Proc. Natl. Acad. Sci. USA* **2020**, *117*, 5895–5906.
[5] a) Z. A. Ripstein, S. Vahidi, J. L. Rubinstein, L. E. Kay, *J. Am. Chem. Soc.* **2020**, *142*, 20519–20523; b) L. Kim, B. G. Lee, M. Kim, M. K. Kim, D. H. Kwon, H. Kim, H. Brötz-Oesterhelt, S. H. Roh, H. K. Song, *EMBO J.* **2022**, *41*, e109755.
[6] a) I. T. Malik, H. Brötz-Oesterhelt, *Nat. Prod. Rep.* **2017**, *34*, 815–831; b) F. Ye, J. Zhang, H. Liu, R. Hilgenfeld, R. Zhang, X. Kong, L. Li, J. Lu, X. Zhang, D. Li, H. Jiang, C.-G. Yang, C. Luo, *J. Biol. Chem.* **2013**, *288*, 17643–17653; c) M. Gersch, A. List, M. Groll, S. A. Sieber, *J. Biol. Chem.* **2012**, *287*, 9484–9494; d) S. R. Geiger, T. Böttcher, S. A. Sieber, P. Cramer, *Angew. Chem. Int. Ed.* **2011**, *50*, 5749–5752.
[7] H. Brötz-Oesterhelt, A. Vorbach, *Front. Mol. Biosci.* **2021**, *8*, 690902.
[8] a) S. Jacques, A. M. Van Der Sloot, C. C. Huard, J. Coulombe-Huntington, S. Tsao, S. Tollis, T. Bertomeu, E. J. Culp, D. Pallant, M. A. Cook, E. Bonneil, P. Thibault, G. D. Wright, M. Tyers, *Genetics* **2020**, *214*, 1103–1120; b) B. G. Lee, E. Y. Park, K. E. Lee, H. Jeon, K. H. Sung, H. Paulsen, H. Rubsamen-Schaeff, H. Brotz-Oesterhelt, H. K. Song, *Nat. Struct. Mol. Biol.* **2010**, *17*, 471–478; c) D. H. Li, Y. S. Chung, M. Gloyd, E. Joseph, R. Ghirlando, G. D. Wright, Y. Q. Cheng, M. R. Maurizi, A. Guarne, J. Ortega, *Chem. Biol.* **2010**, *17*, 959–969; d) J. Kirstein, A. Hoffmann, H. Lilie, R. Schmidt, H. Rübsamen-Waigmann, H. Brötz-Oesterhelt, A. Mogk, K. Turgay, *EMBO Molecular Medicine* **2009**, *1*, 37–49.
[9] a) T. Böttcher, S. A. Sieber, *J. Am. Chem. Soc.* **2008**, *130*, 14400–14401; b) T. Böttcher, S. A. Sieber, *ChemBioChem* **2009**, *10*, 663–666; c) M. Gersch, F. Gut, V. S. Korotkov, J. Lehmann, T. Böttcher, M. Rusch, C. Hedberg, H. Waldmann, G. Klebe, S. A. Sieber, *Angew. Chem. Int. Ed.* **2013**, *52*, 3009–3014.
[10] a) K. A. Gill, F. Berrué, J. C. Arens, G. Carr, R. G. Kerr, *J. Nat. Prod.* **2015**, *78*, 822–826; b) F. Wolf, J. S. Bauer, T. M. Bendel, A. Kulik, J. Kalinowski, H. Gross, L. Kaysser, *Angew. Chem. Int. Ed.* **2017**, *56*, 6665–6668; c) D. Niroula, L. P. Hallada, C. Le Chapelain, S. K. Ganegamage, D. Dotson, S. Rogelj, M. Groll, R. Tello-Aburto, *Eur. J. Med. Chem.* **2018**, *157*, 962–977.
[11] M. Gersch, R. Kolb, F. Alte, M. Groll, S. A. Sieber, *J. Am. Chem. Soc.* **2014**, *136*, 1360–1366.
[12] M. H. Wright, S. A. Sieber, *Nat. Prod. Rep.* **2016**, *33*, 681–708.
[13] C. S. Lentz, J. R. Sheldon, L. A. Crawford, R. Cooper, M. Garland, M. R. Amieva, E. Weerapana, E. P. Skaar, M. Bogyo, *Nat. Chem. Biol.* **2018**, *14*, 609–617.
[14] D. Frees, S. N. A. Qazi, P. J. Hill, H. Ingmer, *Mol. Microbiol.* **2003**, *48*, 1565–1578.
[15] A. Michel, F. Agerer, C. R. Hauck, M. Herrmann, J. Ullrich, J. Hacker, K. Ohlsen, *J. Bacteriol.* **2006**, *188*, 5783–5796.
[16] M. Gominet, N. Seghezzi, P. Mazodier, *Microbiology* **2011**, *157*, 2226–2234.
[17] C. L. Compton, K. R. Schmitz, R. T. Sauer, J. K. Sello, *ACS Chem. Biol.* **2013**, *8*, 2669–2677.
[18] H. B. Bürgi, J. D. Dunitz, E. Shefter, *J. Am. Chem. Soc.* **1973**, *95*, 5065–5067.
[19] A. Szyk, M. R. Maurizi, *J. Struct. Biol.* **2006**, *156*, 165–174.
[20] M. L. Stein, H. Cui, P. Beck, C. Dubiella, C. Voss, A. Krüger, B. Schmidt, M. Groll, *Angew. Chem. Int. Ed.* **2014**, *53*, 1679–1683.
[21] a) M. W. Hackl, M. Lakemeyer, M. Dahmen, M. Glaser, A. Pahl, K. Lorenz-Baath, T. Menzel, S. Sievers, T. Böttcher, I. Antes, H. Waldmann, S. A. Sieber, *J. Am. Chem. Soc.* **2015**, *137*, 8475–8483; b) M. Schwarz, I. Hübner, S. A. Sieber, *ChemBioChem* **2022**, *23*, e202200253; c) E. J. Culp, D. Sychantha, C. Hobson, A. C. Pawlowski, G. Prehna, G. D. Wright, *Nat. Microbiol.* **2022**, *7*, 451–462.
[22] a) E. C. Griffith, Y. Zhao, A. P. Singh, B. P. Conlon, R. Tangallapally, W. R. Shadrick, J. Liu, M. J. Wallace, L. Yang, J. M. Elmore, Y. Li, Z. Zheng, D. J. Miller, M. N. Cheramie, R. B. Lee, M. D. LaFleur, K. Lewis, R. E. Lee, *ACS Infect. Dis.* **2019**, *5*, 1915–1925; b) P. R. Graves, L. J. Aponte-Collazo, E. M. J. Fennell, A. C. Graves, A. E. Hale, N. Dicheva, L. E. Herring, T. S. K. Gilbert, M. P. East, I. M. McDonald, M. R. Lockett, H. Ashamalla, N. J. Moorman, D. S. Karanewsky, E. J. Iwanowicz, E. Holmuhamedov, L. M. Graves, *ACS Chem. Biol.* **2019**, *14*, 1020–1029; c) J. Ishizawa, S. F. Zarabi, R. E. Davis, O. Halgas, T. Nii, Y. Jitkova, R. Zhao, J. St-Germain, L. E. Heese, G. Egan, V. R. Ruvolo, S. H. Barghout, Y. Nishida, R. Hurren, W. Ma, M. Gronda, T. Link, K. Wong, M. Mabanglo, K. Kojima, G. Borthakur, N. MacLean, M. C. J. Ma, A. B. Leber, M. D. Minden, W. Houry, H. Kantarjian, M. Stogniew, B. Raught, E. F. Pai, A. D. Schimmer, M. Andreeff, *Cancer Cell* **2019**, *35*, 721–737.e729; d) C. R. Viera, B. T. Stevens, T. Viera, C. Zielinski, L. A. Uranga, S. Rogelj, P. L. Patidar, R. Tello-Aburto, *R. Soc. Open Sci.* **2022**, *9*, 220358.
[23] V. Bhandari, K. S. Wong, J. L. Zhou, M. F. Mabanglo, R. A. Batey, W. A. Houry, *ACS Chem. Biol.* **2018**, *13*, 1413–1425.

Manuscript received: September 19, 2023
Accepted manuscript online: November 29, 2023
Version of record online: December 12, 2023